



Chinese Pharmaceutical Association  
Institute of Materia Medica, Chinese Academy of Medical Sciences

Acta Pharmaceutica Sinica B

[www.elsevier.com/locate/apsb](http://www.elsevier.com/locate/apsb)  
[www.sciencedirect.com](http://www.sciencedirect.com)



ORIGINAL ARTICLE

# Dual alarmin-receptor-specific targeting peptide systems for treatment of sepsis



Seok-Jun Mun<sup>a,b,†</sup>, Euni Cho<sup>a,b,†</sup>, Woo Jin Gil<sup>b,c,†</sup>, Seong Jae Kim<sup>c</sup>,  
Hyo Keun Kim<sup>b,c</sup>, Yu Seong Ham<sup>b,c</sup>, Chul-Su Yang<sup>c,d,\*</sup>

<sup>a</sup>Department of Bionano Engineering, Hanyang University, Seoul 04673, Republic of Korea

<sup>b</sup>Center for Bionano Intelligence Education and Research, Ansan 15588, Republic of Korea

<sup>c</sup>Department of Molecular and Life Science, Hanyang University, Ansan 15588, Republic of Korea

<sup>d</sup>Department of Medicinal and Life Science, Hanyang University, Ansan 15588, Republic of Korea

Received 13 March 2024; received in revised form 1 August 2024; accepted 13 August 2024

## KEY WORDS

Sepsis;  
High mobility group box 1;  
Pentraxin 3;  
Liposome;  
Antibiotics

**Abstract** The pathophysiology of sepsis is characterized by a systemic inflammatory response to infection; however, the cytokine blockade that targets a specific early inflammatory mediator, such as tumor necrosis factor, has shown disappointing results in clinical trials. During sepsis, excessive endotoxins are internalized into the cytoplasm of immune cells, resulting in dysregulated pyroptotic cell death, which induces the leakage of late mediator alarmins such as HMGB1 and PTX3. As late mediators of lethal sepsis, overwhelming amounts of alarmins bind to high-affinity TLR4/MD2 and low-affinity RAGE receptors, thereby amplifying inflammation during early-stage sepsis. In this study, we developed a novel alarmin/receptor-targeting system using a TLR4/MD2/RAGE-blocking peptide (TMR peptide) derived from the HMGB1/PTX3-receptors interacting motifs. The TMR peptide successfully attenuated HMGB1/PTX3- and LPS-mediated inflammatory cytokine production by impairing its interactions with TLR4 and RAGE. Moreover, we developed TMR peptide-conjugated liposomes (TMR-Lipo) to improve the peptide pharmacokinetics. In combination therapy, moderately antibiotic-loaded TMR-Lipo demonstrated a significant therapeutic effect in a mouse model of cecal ligation- and puncture-induced sepsis. The identification of these peptides will pave the way for the development of novel pharmacological tools for sepsis therapy.

© 2024 The Authors. Published by Elsevier B.V. on behalf of Chinese Pharmaceutical Association and Institute of Materia Medica, Chinese Academy of Medical Sciences. This is an open access article under the CC BY-NC-ND license (<http://creativecommons.org/licenses/by-nc-nd/4.0/>).

\*Corresponding author.

E-mail address: [chulsuyang@hanyang.ac.kr](mailto:chulsuyang@hanyang.ac.kr) (Chul-Su Yang).

<sup>†</sup>These authors made equal contributions to this work.

Peer review under the responsibility of Chinese Pharmaceutical Association and Institute of Materia Medica, Chinese Academy of Medical Sciences.

<https://doi.org/10.1016/j.apsb.2024.08.015>

2211-3835 © 2024 The Authors. Published by Elsevier B.V. on behalf of Chinese Pharmaceutical Association and Institute of Materia Medica, Chinese Academy of Medical Sciences. This is an open access article under the CC BY-NC-ND license (<http://creativecommons.org/licenses/by-nc-nd/4.0/>).

## 1. Introduction

Sepsis is a clinical syndrome characterized by systemic inflammation caused by infection and is associated with substantial mortality (in-hospital mortality rates 30–50%)<sup>1</sup>. In 2016, the Third International Consensus Definitions for Sepsis and Septic Shock (Sepsis-3) defined sepsis as “organ dysfunction resulting from a dysregulated host immune response to infection,” marking the first acknowledgment of the vital role that the innate and adaptive immune response plays in sepsis pathophysiology<sup>2</sup>. Sepsis pathophysiology is characterized by a hyperinflammatory phase with systemic activation of the innate immune system<sup>3</sup>. The initial stages of sepsis involve host recognition of microbial-derived pathogen-associated molecular patterns (PAMPs) such as endotoxins or endogenous damage-associated molecular patterns (DAMPs), which are affirmed by pattern recognition receptors (PRRs) predominantly expressed on immune cell surfaces<sup>4</sup>. The recognition initiates host intracellular signaling, which converges toward early activation genes such as interferon regulatory factor (IRF) and nuclear factor- $\kappa$ B (NF- $\kappa$ B). Overall, this systemic activation of the innate immune system by PAMPs and DAMPs perpetuate inflammatory response, marked by an uncontrolled release of inflammatory cytokines, including TNF- $\alpha$ , IL-1, IL-6, and IL-10, known as the “cytokine storm,” which results in organ dysfunction as well as increased susceptibility to septic shock<sup>5,6</sup>.

Although therapeutic interventions involving cytokine and receptor blockades have shown promise in preclinical settings, clinical trials have yielded disappointing results<sup>7</sup>. For instance, clinical trials have shown that TNF antagonists are most effective in chronic inflammatory conditions such as rheumatoid arthritis but have exhibited limited efficacy in patients with sepsis. This is likely because these cytokines serve as “early proinflammatory mediators” in the pathogenesis of sepsis. Indeed, the release of TNF- $\alpha$  occurs within mins after LPS exposure<sup>8</sup>, which makes timely intervention far too challenging in sepsis therapy. Therefore, therapeutic approaches targeting potential late mediators of sepsis might be beneficial for septic patients.

Recent findings that alarmins are pivotal mediators of sepsis pathophysiology provide valuable insights into the modulation of septic responses. As best characterized alarmins, high-mobility group protein B1 (HMGB1) and pentraxin 3 (PTX3) are late mediators of endotoxemia and sepsis, which are rapidly released into the circulation by injured organs and tissue<sup>9</sup>. These alarmins serve as innate amplifiers of infection through alarmin-PRR interactions, and their release is accompanied by the upregulation of their cognate receptors. For instance, the toll-like receptor 4 (TLR4)/myeloid differentiation factor 2 (MD-2) complex and receptor for advanced glycation end products (RAGE) have been shown to fuel the innate inflammatory response by interacting with these alarmins in septic shock, and their inhibition offers a protective effect in polymicrobial sepsis models<sup>10</sup>. Moreover, these alarmins appear to act as late-stage mediators of sepsis<sup>8,11</sup>, offering a clinically relevant timeframe for pharmacological intervention by targeting the alarmin-receptor axis. Thus, interrupting the inflammatory feedback loop resulting from an exaggerated alarmin/PRR axis impedes inflammation and restores a physiologically appropriate immune response to infection.

In this study, we developed a novel alarmin/PRR-targeted system using a TLR4/MD2/RAGE-targeted peptide (TMR peptide) derived from the HMGB1, PTX3-TLR4/MD2, or RAGE-

interacting domains. The TMR peptide was further functionalized by conjugation with liposomes (TMR-Lipo), a liposomal delivery system, to improve its unfavorable pharmacokinetic properties. We demonstrated that TMR-Lipo suppressed TLR4- and RAGE-mediated inflammation by blocking the alarmin-PRR axis in LPS-treated macrophages. Most importantly, the combination of TMR-lipo and antibiotics, which possess both immunomodulatory and antimicrobial capacities, significantly affected the survival of CLP-induced septic mice by targeting the alarmin-PRR axis, thus mitigating exacerbated inflammation. This synergistic therapeutic approach involving antibiotics and TMR-lipo holds great promise as a therapeutic strategy for sepsis.

## 2. Materials and methods

### 2.1. Mice and cell culture

Primary bone marrow-derived macrophages (BMDMs) were isolated from female C57BL/6 mice and cultured for 5–7 days in media supplemented with M-CSF for differentiation. HEK293T cells were acquired from the American Type Culture Collection (ATCC). Both BMDMs and HEK293T cells were nurtured in Dulbecco’s modified Eagle’s medium (DMEM, GenDEPOT, USA) supplemented with 10% FBS, penicillin (100 U/mL), and streptomycin (100  $\mu$ g/mL).

Wild-type female C57BL/6 mice were obtained from Samtako Bio Korea (Osan, Republic of Korea) and housed under standard conditions at the Center for Laboratory Animal Science at Hanyang University (Ansan, Republic of Korea). All animal breeding and experimental procedures were conducted in accordance with the guidelines approved by the IACUC of Hanyang University (protocol 2022-0004).

### 2.2. Plasmid construction

Flag-HMGB1 (MG50913-CF), Flag-PTX3 (HF12082-CF), HA-TLR4 (MG50657-NY), Myc-RAGE (MG50489-CM), and His-MD2 (MG51098-NH) plasmids were purchased from Sino Biological (Beijing, China). Plasmids encoding different regions of HMGB1 or PTX3 were produced by PCR amplification of full-length HMGB1 or PTX3 cDNA and subcloned into a pEBG derivative encoding an N-terminal GST epitope tag positioned between the BamHI and NotI sites. All the constructs were sequenced to confirm an absolute match with 100% correspondence to the original sequence.

### 2.3. Recombinant protein

To acquire recombinant rFlag-HMGB1, rFlag-PTX3, rHA-TLR4, rMyc-RAGE, and rHis-MD2 were cloned with an N-terminal tag into a pRSFDuet-1 vector (Novagen, USA). Subsequently, this was performed by expressing, harvesting, and purifying BL21(DE3) pLysS, as outlined previously<sup>12</sup>, following the standard procedures recommended by Novagen. The purified rFlag-HMGB1, rFlag-PTX3, rHA-TLR4, rMyc-RAGE, and rHis-MD2 were dialyzed with a permeable cellulose membrane, examined for lipopolysaccharide contamination using a limulus amoebocyte lysate assay (BioWhittaker), and demonstrated to contain <20 pg/mL lipopolysaccharide.

#### 2.4. Peptides

HMGB1 and PTX3 peptides were industrially synthesized and purified in acetate salt form by Lugen Science (Republic of Korea) to prevent abnormal reactions in cells. The peptide sequences used in this study are shown in Figs. 2A, B, and 3A. The purification and identification data of industrial synthesized HMGB1 and PTX3 peptides in Supporting Information Fig. S1.

#### 2.5. GST pulldown and immunoprecipitation analyses

HEK293T cells and BMDM were treated as specified and processed for analysis using GST pulldown and co-immunoprecipitation assays. For GST pulldown, HEK293T cells were harvested and lysed in RIPA buffer containing a complete protease inhibitor cocktail (GenDEPOT). Following centrifugation, the supernatants were mixed with a 50% slurry of glutathione-conjugated Sepharose beads (Amersham Biosciences, Amersham, UK), and incubated for 1 h at 4 °C. The precipitate was washed repeatedly with RIPA buffer. Proteins bound to glutathione beads were eluted with sodium dodecyl sulfate (SDS) buffer by boiling for 5 min. For immunoprecipitation, HEK293T cells and BMDM were harvested and lysed in RIPA buffer containing a complete protease inhibitor cocktail (GenDEPOT, USA). After pre-clearing with protein A/G agarose beads for 1 h at 4 °C, lysates were utilized for immunoprecipitation with the specified antibodies. Typically, 1–4 µg of commercially available antibody was introduced to 1 mL of cell lysates and incubated at 4 °C overnight. After adding protein A/G agarose beads for 2 h, the immunoprecipitants were repeatedly washed with RIPA buffer and eluted with SDS buffer by boiling for 5 min.

#### 2.6. Immunoblotting

For immunoblotting, the proteins were resolved by SDS-PAGE and transferred onto a polyvinylidene difluoride (PVDF) membrane (IPVH00010, Merck, USA). Anti-HMGB1 (ab228624), Anti-TLR4 (ab95562) and Anti-KRAS (ab206969) were purchased from Abcam, UK. Anti-Flag (2368S), Anti-HA (3724S), Anti-Myc (2278S), Anti-His (12698S) and Anti-GST (2625S) were purchased from Cell Signaling Technology (CST, USA). Anti-PTX3 (sc-373951), Anti-RAGE (sc-365154), Anti-MyD88 (sc-74532), Anti-TRAF6 (sc-8409), Anti-IRAK (sc-5288), Anti-NF-κB (sc-372), Anti-β-Actin (sc-47778), and Anti-GAPDH (sc-32233) were purchased from SANTA CRUZ BIOTECHNOLOGY, USA. Anti-p-p38 MAPK (MA5-15182) and Anti-MD2 (MA5-15766) were purchased from Invitrogen, USA. The membranes were incubated overnight at 4 °C. Antibody conjugation was visualized using EzWestLumi Plus (ATTO, Japan) and detected using a Vilber chemiluminescence analyzer (Fusion Solo; Vilber Lourmat, France).

#### 2.7. Enzyme-linked immunosorbent assay

Supernatants of cultured BMDMs and serum of CLP-induced mice were measured for cytokine content using the Uncoated ELISA Kit for the detection of TNF-α (88-7324-88, Invitrogen, USA), IL-6 (88-7064-88, Invitrogen), IL-10 (88-7105-88, Invitrogen). The IL-12p40 cytokine was measured using the OptEIA™ Mouse IL-12 p40 ELISA Set (555165, BD Biosciences, USA). All experiments were conducted following the guidelines provided by the manufacturer.

#### 2.8. In vitro cell viability study

BMDMs were seeded in 96-well plates (SPL, Republic of Korea) at a density of  $2 \times 10^4$  cells/well and incubated in complete DMEM for 18 h. Subsequently, the cells were treated with various concentrations of H-T, H-R, P-T, P-M peptide, control, TMR, or TMR using Abs Lipo. After 48 h of incubation, the medium was replaced with 100 µl of DMEM with Quanti-Max solution (10% of each media volume). Following a 2-h incubation at 37 °C and 5% CO<sub>2</sub>, the absorbance of the plates included with Quanti-Max solution was measured at 450 nm using MMR SPARK® microplate reader (TECAN, Switzerland).

#### 2.9. Fabrication and characterization of liposomes

We prepared 0.5 wt% liposomes using the TMR peptide, according to our previous research<sup>13</sup>. DPPC (850355C, Avanti Polar Lipids, USA) and PEG (81188; Sigma-Aldrich) were dissolved in chloroform in a round-bottomed flask. The mixing ratio of DPPC to PEG was adjusted to 9:1, and the concentration of the TMR peptide was set to 1 mM. For peptide conjugation, PEG and DSPE-PEG<sub>2000</sub>-maleimide (880126C, Avanti Polar Lipids, USA) were mixed at a ratio of 75:25<sup>14,15</sup>. Subsequently, the solvent was evaporated in a rotary evaporator at 42 °C for 90 min to generate a thin film at the bottom of the flask. PBS was then added to the round-bottomed flask and the film was hydrated in a water sonicator at 42 °C for 90 min.

To encapsulate the antibiotics, Ampicillin (AMP 25, LPS solution, Republic of Korea) and Gentamicin (GENT025, LPS solution, Republic of Korea) were dissolved in PBS and each concentration of Amp and Gen was set to 30 and 2 mmol/L<sup>16-18</sup>.

To conjugate the TMR peptide with the maleimide co-assembled with the vesicular membrane, TMR-cysteamide was added to the liposome, and mixture was rotated at 4 °C for overnight. The hydrodynamic particle size of control liposome (C-Lipo), TMR liposome (TMR-Lipo) and TMR liposome with antibiotics (TMR-Lipo-Abs) were confirmed by dynamic light scattering (DLS 1070, Malvern, United Kingdom) at 25 °C. The morphologies of C-Lipo, TMR-Lipo, and TMR-Lipo-Abs were observed using a transmission electron microscope (JEM 1010, JEOL, Japan).

To determine the conjugated rate of TMR-Lipo and the encapsulated TMR-Lipo-Abs, fluorescein isothiocyanate (FITC) was equimolarly conjugated to the TMR peptide or Abs (TMR peptide-FITC, Abs-FITC) using the FluoroTag™ FITC Conjugation Kit (FITC1, Merck, USA). Using the above method, liposomes containing TMR peptide-FITC conjugates or Abs-FITC conjugates were produced at various concentrations. The prepared liposomes were centrifuged at 27,000 × g for 2 h to separate the liposome pellet from the supernatant, and the level of residual TMR peptide-FITC or Abs-FITC in each supernatant was measured. The fluorescence intensity of the TMR peptide-FITC or Abs-FITC standard was measured using a microplate reader in the range of 485 nm to 535 nm. Finally, the conjugation efficiency and encapsulation efficiency were calculated with the following Eqs. (1) and (2):

$$\text{Conjugation efficiency (\%)} = (1 - (\text{TMR peptide-FITC in supernatant}/\text{total TMR peptide-FITC})) \times 100 \quad (1)$$

$$\text{Encapsulation efficiency (\%)} = (1 - (\text{Antibiotics-FITC in supernatant}/\text{total Antibiotics-FITC})) \times 100 \quad (2)$$

A Malvern Zetasizer Nano ZS90 (Malvern Instruments Ltd., UK) was used to determine the mean size, polydispersity index (PDI), and zeta potential of different liposomes. The morphology of liposome was examined by transmission electron microscopy (Tecnai G2 F20 S-Twin; FEI, Hillsboro, OR, USA). Liposome stability was evaluated by monitoring and the mean size, PDI at 4 °C for 8 days.

### 2.10. Sepsis modeling in mice

Cecal ligation and puncture (CLP) was performed on 6-week-old C57BL/6 female mice following previously established protocols<sup>19</sup>. To perform CLP, mice were anesthetized with 2,2,2-tribromoethanol (250 mg/kg, i.p.), and a small midline incision was made in the abdominal region to expose the cecum. The cecum was ligated below the ileocecal valve, punctured twice through both surfaces using a 22-gauge needle, and the abdominal incision was closed. In this study, we induced sepsis in two groups: mid-grade and high-grade. In the mid-grade group, after modeling, liposomes were administered intraperitoneally three times at 1-, 12-, and 48-h post-modeling. In the high-grade group, liposomes were administered either intraperitoneally or subcutaneously at 1- and 12-h post-modeling. Ampicillin (Amp) and Gentamicin (Gen) were administered at doses of 50 mg/kg and 3 mg/kg<sup>20,21</sup>, respectively. TMR peptide was administered at doses of 0.5 or 2 mg/kg. Survival rate was monitored daily for 3 and 10 days.

### 2.11. Histology

For the immunohistochemical analysis of mouse tissues, the lungs, liver, and spleen were fixed in 10% formalin and subsequently embedded in paraffin. Paraffin sections (4 µm) were prepared and subjected to hematoxylin and eosin (H&E) staining. The histopathological score was determined based on the distribution and severity of inflammation within the tissues and cells. A board-certified pathologist independently confirmed each tissue section without prior knowledge of the group.

### 2.12. In vivo bio-distribution of TMR-Lipo in the nude mice

*In vivo* bio-distribution of TMR-Lipo with IR783 in the nude mice was observed *via* the IVIS Spectrum-CT *in vivo* imaging system (PerkinElmer, USA). TMR-Lipo (0.5 mg/kg, 100 µL) was injected intraperitoneally into nude mice. After the injection, time-dependent whole body NIRF imaging was performed up to 48 h post-injection.

### 2.13. Statistical analysis

All data are presented as mean ± SD or SEM and were assessed using the Student's t-test with a Bonferroni adjustment or ANOVA for multiple comparisons. Statistical analyses were performed using GraphPad Prism software (version 8.0; La Jolla, CA, USA). Differences were considered statistically significant at  $P < 0.05$ . Survival data were analyzed and visualized using the Kaplan–Meier product limit method with the log-rank (Mantel-Cox) test for comparisons using GraphPad Prism.

## 3. Result

### 3.1. Alarmins HMGB1 and PTX3 enhance inflammation in TLR4/RAGE-mediated signaling through its interaction with their receptor

HMGB1 and PTX3 are ubiquitously expressed alarmins released from immune cells during the septic response<sup>22</sup>. Macrophages are key innate immune players and are a major source of cytokines upon activation by LPS<sup>23</sup>. We stimulated murine bone marrow-derived macrophages (BMDMs) with lipopolysaccharide (LPS) in a time-dependent manner and analyzed HMGB1 and PTX3 secretion by immunoblotting. In LPS-stimulated BMDMs, the intracellular expression of HMGB1 and PTX3 increased after approximately 2 to 4 h, with pronounced secretion occurring approximately 12 h later (Fig. 1A and B). As the alarmin-PRR axis is critically involved in sepsis pathology, we further investigated whether HMGB1 and PTX3 physically interact with TLR4 or RAGE by co-immunoprecipitation and whether this interaction contributes to inflammatory responses. In HEK293T cells, over-expressed Flag-HMGB1 interacted with both HA-TLR4 and Myc-RAGE (Fig. 1C, left panel). Moreover, recombinant Flag-HMGB1 interacted with both endogenous TLR4 and RAGE in the BMDM (Fig. 1C, right panel). Regarding PTX3, previous studies have reported its interaction with the TLR4/MD2 complex but not with RAGE<sup>24</sup>. Validation of this interaction by co-immunoprecipitation showed that ectopically expressed Flag-PTX3 interacted with the TLR4/MD2 complex in HEK293T cells (Fig. 1D, left panel), and recombinant Flag-PTX3 also interacted with endogenous TLR4/MD2 in BMDM (Fig. 1D, right panel), consistent with previous studies. To determine whether the physical interactions between these alarmins and PRRs are functionally relevant to their roles in the inflammatory response, we assessed the levels of proinflammatory cytokines induced by the activation of TLR4 and RAGE signaling by stimulating murine BMDM with LPS or recombinant alarmin proteins (rHMGB1 or rPTX3).

rHMGB1 or rPTX3-treated BMDMs showed elevated levels of proinflammatory cytokines, including TNF- $\alpha$ , IL-6, and IL-12p40, as well as anti-inflammatory cytokine IL-10, a slightly lower degree of expression compared to LPS alone (Fig. 1E). Notably, combining LPS with rHMGB1 or rPTX3 significantly increased the production of these cytokines compared with LPS alone. These findings suggest that alarmin proteins contribute to the amplification of sterile inflammation. Collectively, extracellular HMGB1 or PTX3 amplified inflammatory responses by interacting with their cognate receptors TLR4 and RAGE in LPS-treated BMDMs.

### 3.2. The inhibitory effects of HMGB1/PTX3-derived peptides on the TLR4/RAGE signaling

Our data suggest that HMGB1 interacts with TLR4 and RAGE, and that PTX3 interacts with TLR4/MD2, which amplifies inflammatory responses under LPS treatment. Previous studies have revealed that HMGB1 has two distinct binding regions within its domain: one for TLR4 binding (residues 89-108) and the other for RAGE binding (150-183)<sup>25</sup>. To further identify the amino regions of HMGB1 essential for TLR4 or RAGE interactions, we performed GST pulldown analyses in HEK293T cell lysates expressing GST-tagged HMGB1 and its binding regions. We found that aa 89-98 of HMGB1 were essentially required for

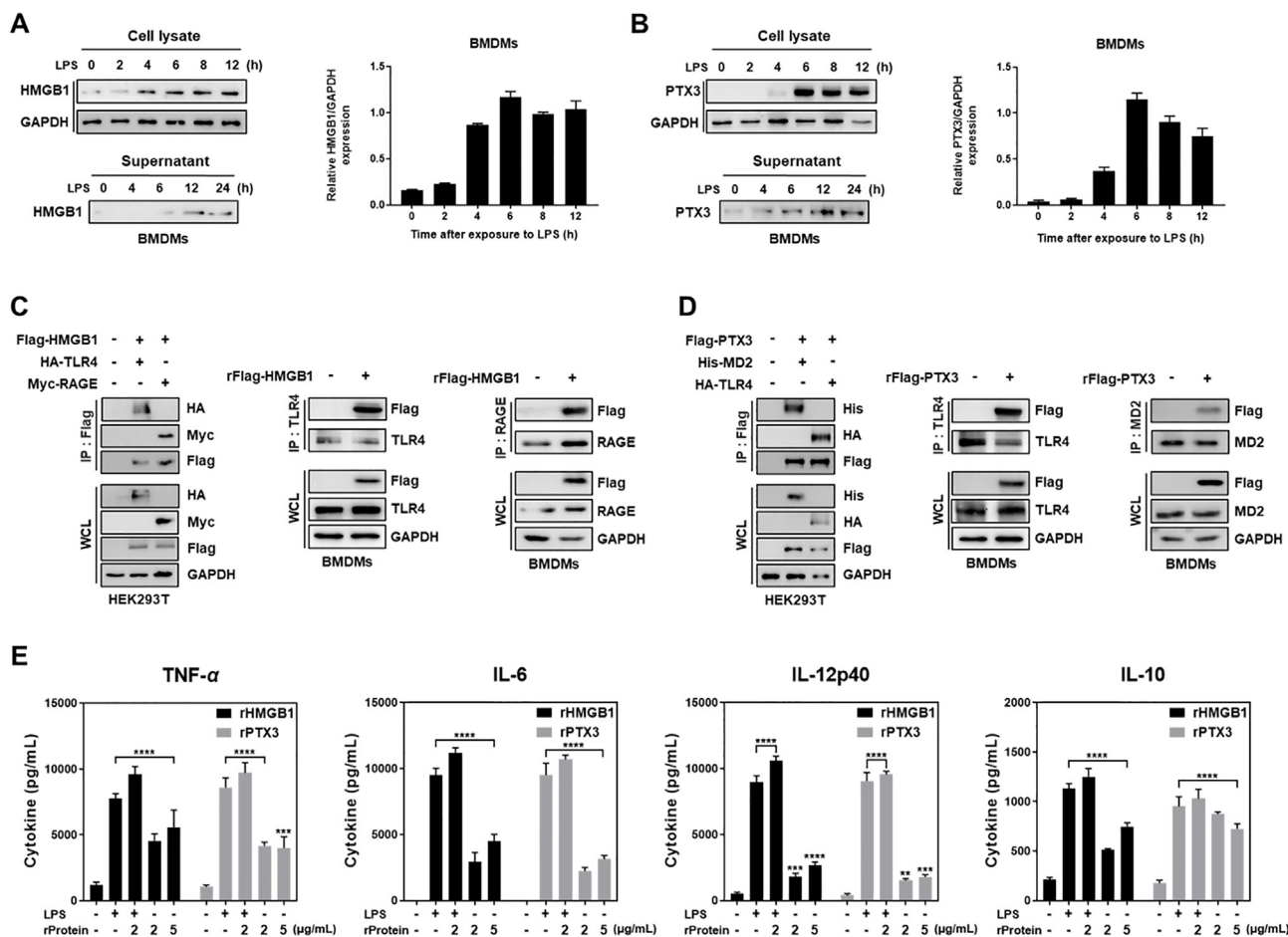


**Figure 1** Extracellular HMGB1 and PTX3 contribute to inflammatory responses by interacting with TLR4 or RAGE in murine macrophages. (A, B) Release of HMGB1 (A) or PTX3 (B) from murine macrophages after stimulation with LPS. LPS-induced HMGB1 (A) or PTX3 (B) release from murine macrophages. Immunoblots (IB) for HMGB1 and PTX3 in the supernatant and cell lysates in LPS-treated BMDMs at indicated time points after LPS (100 ng/mL). (C, D) Interaction between HMGB1 (C) or PTX3 (D) with its receptors. HEK293T cells were transfected with constructs, and cell lysates were immunoprecipitated with a flag-specific antibody and were analyzed by immunoblotting with the indicated antibodies. BMDMs were incubated with the rFlag-HMGB1 (C) or rFlag-PTX3 (D) 10  $\mu$ g/mL for 3 h, and cell lysates were immunoprecipitated with  $\alpha$ TLR4 or  $\alpha$ RAGE (C, right), and  $\alpha$ TLR4 or  $\alpha$ MD-2 (D, right). Immunoprecipitants and WCL were analyzed by immunoblotting with the indicated antibodies. (E) TNF- $\alpha$ , IL-6, IL-12p40, and IL-10 levels in the supernatant of LPS (100 ng/mL, 18 h) or recombinant alarmins (rHMGB1 or rPTX3, each (2, 5  $\mu$ g/mL))-treated BMDMs determined by ELISA. The data shown represent at least three independent experiments ( $n \geq 3$ ), and bars denote mean  $\pm$  SEM (\*\*\*\* $P < 0.001$ ), significance was measured by two-way ANOVA.

TLR4-binding, while aa 160-169 were essential for RAGE binding (Fig. 2A). Myeloid differentiation protein 2 (MD2), a co-receptor for TLR4, is essential for the PTX3-TLR4 interaction and subsequent TLR4 activation<sup>24</sup>. Thus, to map TLR4 and MD2 binding sites within PTX3, we expressed truncated variants of PTX3 (each truncate comprising 10 aa segments from 18 to 182 regions of PTX3) in HEK293 cells and performed GST pull-downs from cell lysates. Our results showed that aa 108-117 of PTX3 interacted with TLR4, and aa 148-157 interacted with MD2 (Fig. 2B).

We have previously identified critical binding motifs through protein-protein interactions (PPI), demonstrating their ability to competitively inhibit receptor binding<sup>26</sup>. This confirms that these fragments play a pivotal role in receptor binding and effectively inhibit the overall protein activity. Based on the potential TLR4-, MD2-, and RAGE-interacting motifs identified in each alarmin, we hypothesized that these motifs could compete with their parent alarmins for PRR binding, thereby

reducing downstream inflammatory responses. To test this hypothesis, we synthesized antagonistic peptides against each PRR based on the sequence of TLR4-, MD2-, and RAGE-interacting motifs (designated H-T, H-R, P-T, and P-M peptides). The synthesized peptides had negligible impact on the viability of BMDM (Fig. 2C). These peptides successfully blocked alarmin-PRR interactions by cell-free immunoprecipitation assay (Fig. 2D). Furthermore, these peptides inhibited the binding of recombinant HMGB1 or PTX3 to their cognate receptors, which are endogenously expressed in macrophages (Fig. 2E). Simultaneously, the antagonistic effect of these peptides on blocking alarmin-PRR interactions resulted in a reduction in the production of inflammatory cytokines, with no observable changes in IL-10 levels (Fig. 2F). Notably, we performed an *in vitro* binding assay with fluorescently labeled HMGB1 and PTX3 and unlabeled peptide of TLR4, RAGE or MD2 to examine the binding affinity differences between HMGB1 and PTX3 to TLR4, RAGE or MD2. Isothermal

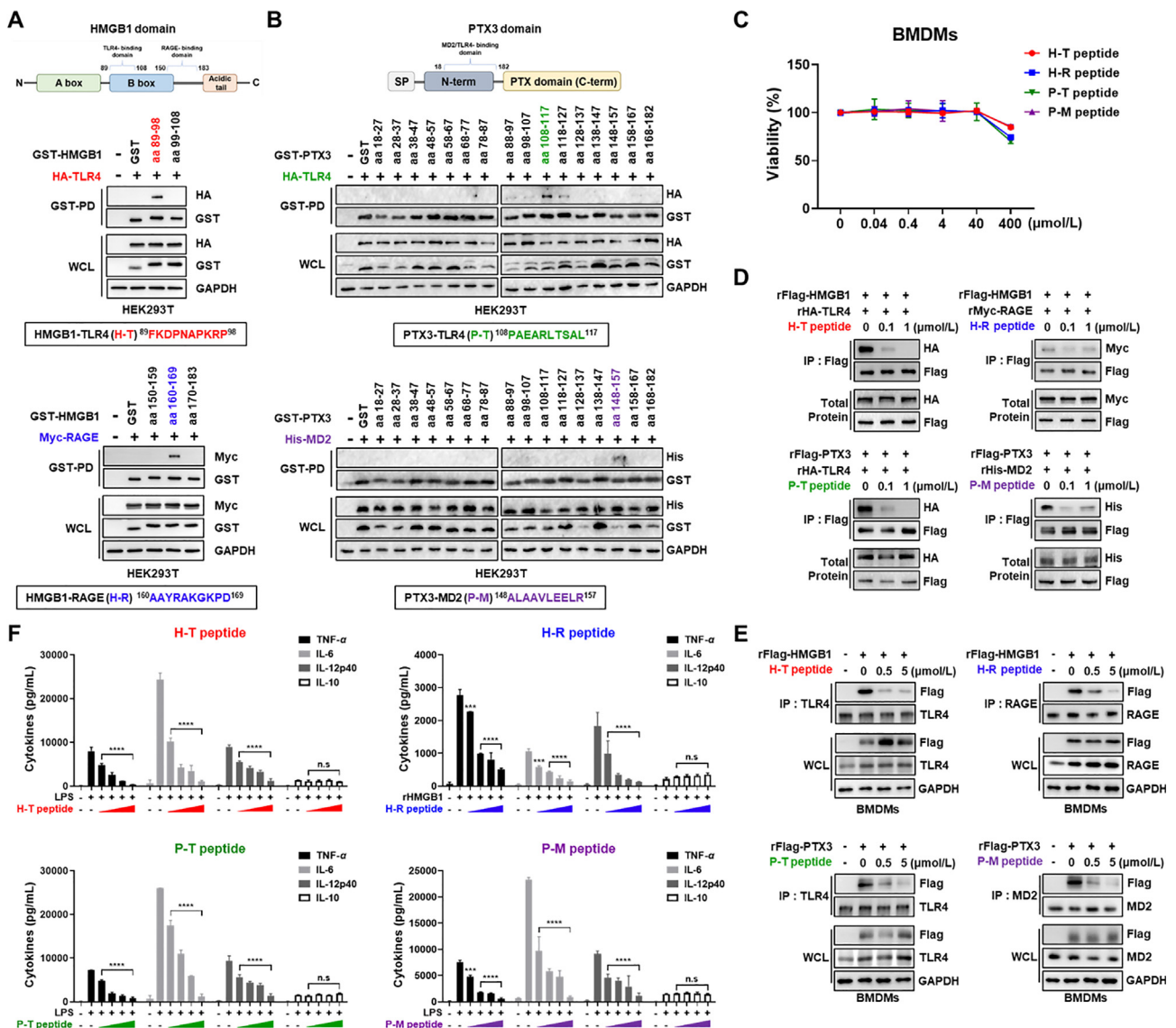


**Figure 2** Mapping of the TLR4/MD2/RAGE-interacting motifs of HMGB1 or PTX3. (A, B) Schematic diagram of the domain of HMGB1 (A) and PTX3 (B) (top). GST-tagged truncates covering TLR4-, RAGE-, or MD2-binding domain of HMGB1 or PTX3 were constructed. Bottom panel (A, B) depicts GST-pull down of the indicated tagged receptors (HA-TLR4, Myc-RAGE, and His-MD2) with transiently expressed GST-tagged truncates. HEK293T cells transfected with the GST-tagged constructs in combination with HA-TLR4, Myc-RAGE or His-MD2 are indicated followed by GST-pull down. Representative western blots of WCLs and eluates after GST-pull down are shown, using GAPDH as a loading control in WCLs. Based on pulldown binding results, TLR4-, MD2-, and RAGE-targeted peptides were constructed and designated as H-T, H-R, P-T, or P-M peptides (indicated in panels A, B). (C) BMDMs were incubated with H-T, H-R, P-T, or P-M peptide for the indicated concentrations for 48 h, and then cell viability was measured with cell viability assay. Data shown are the means  $\pm$  SD of three experiments (D) Cell-free immunoprecipitation assay using H-T, H-R, P-T, or P-M peptides. Mix 5  $\mu$ g of alarmin protein (rHMGB1 or rPTX3) with 5  $\mu$ g of each indicated tagged receptors protein (HA-TLR4, Myc-RAGE, and His-MD2), and mix as indicated to confirm the competitive inhibition effect of peptides was treated for 4 h. They were immunoprecipitated with  $\alpha$ Flag for 2 h, separated by SDS-PAGE, and evaluated by immunoblotting. (E) Competition between rHMGB1 (top) or PTX3 (bottom) and the constructed peptides for their respective receptors. After treatment with rHMGB1 (top) or PTX3 (bottom) (10  $\mu$ g/mL, 3 h) together with increasing amounts of the indicated peptides, BMDMs were used for immunoprecipitation (IP) with  $\alpha$ TLR4 or  $\alpha$ RAGE and IB with indicated antibodies. (F) Decrease of LPS-induced cytokine production by H-T, P-T, or P-M peptide and rHMGB1-induced cytokine production by H-R peptide. TNF- $\alpha$ , IL-6, IL-12p40, and IL-10 levels in the supernatant of LPS (100 ng/mL, 18 h) together with increasing amounts of the indicated peptides-treated BMDMs were determined by ELISA. The data shown represent at least three independent experiments ( $n \geq 3$ ), bars denote mean  $\pm$  SEM (\*\*\* $P < 0.001$ , \*\*\*\* $P < 0.0001$ ), and significance was measured by two-way ANOVA. n.s. = not significant.

titration calorimetry data clearly showed that HMGB1 or PTX3 with TLR4, RAGE or MD2 was direct interactions and HMGB1 to TLR4 and RAGE binding was stronger than that of PTX3 to TLR4 and MD2 (Supporting Information Fig. S2). These findings indicated that these peptides act as antagonistic peptides against TLR4- and RAGE-mediated signaling.

### 3.3. The inhibitory effects of TMR-Lipo on the alarmin-PRR signaling pathway

In sepsis, alarmin-mediated activation of PRRs, especially TLR4 and RAGE, fuels proinflammatory cytokine production by macrophages and other immune cells, leading to excessive tissue inflammation. We hypothesized that targeting the double alarmin-PRR axis (HMGB1-TLR4/RAGE or PTX3-TLR4/MD2) using TLR4/MD2- and RAGE-interacting motifs may regulate exacerbated inflammatory responses in sepsis. To test our hypothesis, we designed a TLR4/MD2-RAGE multiblocking TMR peptide by covalently conjugating TLR4/MD2 and RAGE-interacting motifs. Based on this peptide, we developed a TMR peptide-tagged liposome (TMR-Lipo) to overcome unfavorable pharmacokinetic properties (Fig. 3A).

Liposomes were prepared using the thin-film hydration method to attain high encapsulation efficiency and well-defined particle size distribution<sup>27</sup>. The characteristic vesicular structure of the C-Lipo and TMR-Lipo was confirmed through transmission electron microscopy (TEM) (Fig. 3B). C-Lipo had an average hydrodynamic particle size of 98.81 nm, and a polydispersity index (PDI) of approximately 0.185. TMR-Lipo showed a hydrodynamic particle size of 99.25 nm, similar to that of C-Lipo, and a PDI value of approximately 0.228 (Fig. 3C). In DSPE-PEG<sub>2000</sub>-maleimide, the hydrophilic maleimide head group is exposed to the aqueous phase<sup>28</sup>, where the thiol-terminated TMR peptide binds *via* thiol-maleimide reaction to produce TMR-Lipo. To determine the conjugation efficiency of the TMR peptide on the surface of liposomes, we normalized the encapsulation efficiency of the TMR peptide in TMR-Lipo by conjugating FITC to the TMR peptide, referring to previous studies<sup>13</sup>. In TMR-Lipo, the encapsulation efficiency of TMR peptide-FITC began to decrease slightly from the concentration of 20 mmol/L of the conjugated TMR peptide; when conjugated in mass units, the encapsulation efficiency decreased from 1 mg. The appropriate concentration of the TMR peptide for conjugation in the preparation of TMR-Lipo was 20 mmol/L (Fig. 3D). Next, we measured

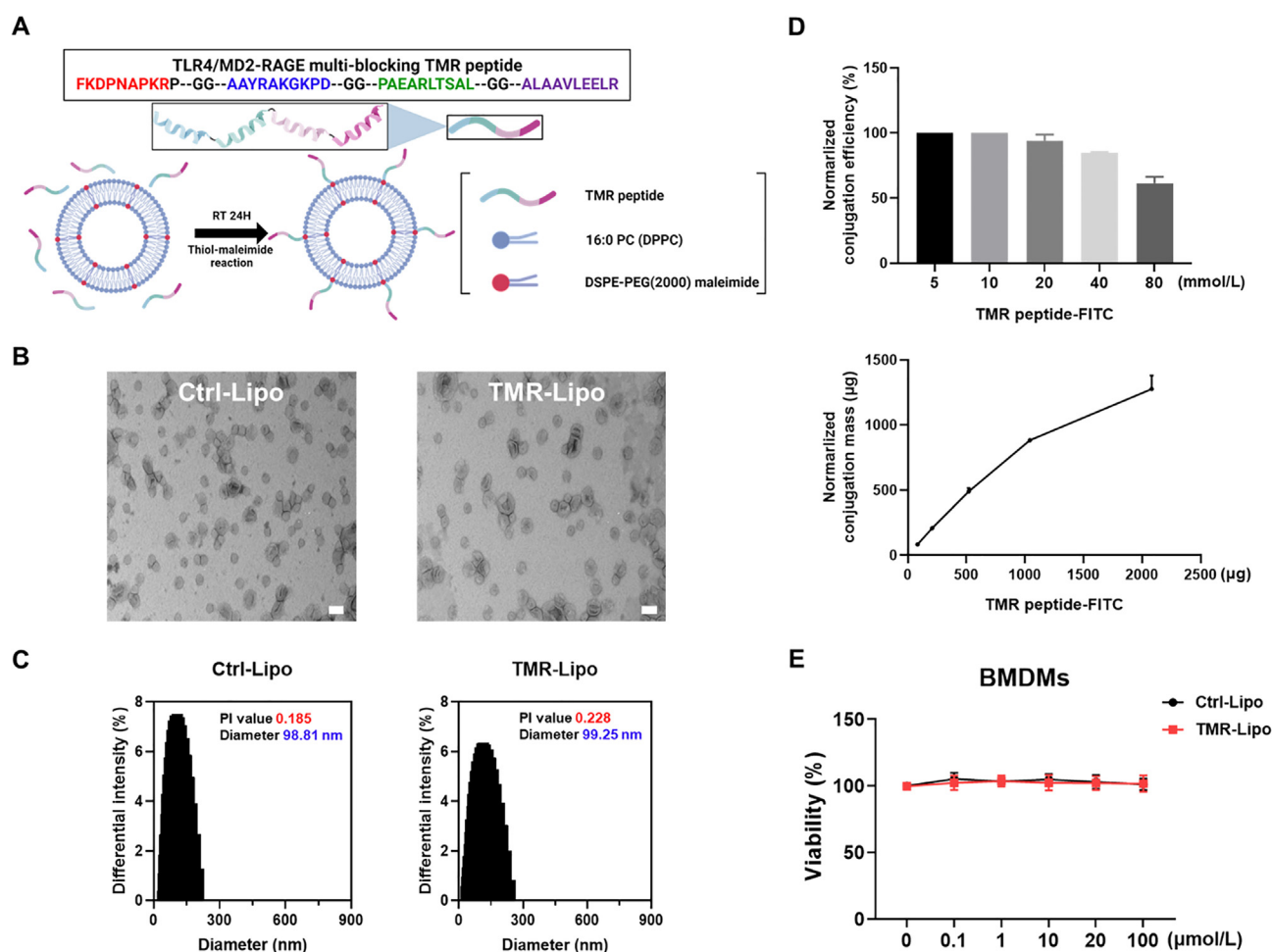


**Figure 3** Preparation and characterization of TMR-Lipo (A) Schematic design of TMR peptide (top) and preparation of TMR-conjugated Liposome (TMR-Lipo) (bottom). (B) TEM image of control liposome (Ctrl-Lipo) and TMR-Lipo. Scale bars are 100 nm. (C) Hydrodynamic particle size of Ctrl-Lipo and TMR-Lipo. (D) Normalized conjugation efficiency of TMR peptide in TMR-Lipo. (E) *In vitro* cell viability of Ctrl-Lipo and TMR-Lipo was evaluated for BMDMs. Data shown are the means  $\pm$  SD of three experiments.

the viability of macrophages treated with C-Lipo or TMR-Lipo. Evaluation of TMR-Lipo viability in a dose-dependent manner confirmed its high biostability in macrophages, similar to that of C-Lipo (Fig. 3E).

Having shown that HMGB1 and PTX3 are released in LPS-treated macrophages and that alarmin-PRR interactions are increased (Fig. 1A–D), we next sought to investigate whether TMR-Lipo might block the endogenous binding of HMGB1 or PTX3 with TLR4 or RAGE in LPS-treated macrophages. To test this, we exposed LPS-primed BMDMs to TMR-Lipo, followed by co-immunoprecipitation with TLR4 or RAGE. As shown in Fig. 4A, the endogenous binding of secreted HMGB1 or PTX3 to their receptors was inhibited in LPS-primed BMDMs upon TMR-Lipo treatment. Inflammatory activation of macrophages by LPS triggers NF- $\kappa$ B activation through TLR4/RAGE signaling and subsequently drives the production of inflammatory cytokines (Fig. 4B). To investigate whether TMR-Lipo regulate TLR4 or RAGE-mediated NF- $\kappa$ B activation and subsequent inflammatory responses, the expression levels of TLR4/RAGE-related downstream signaling molecules were detected by WB analysis in BMDMs after being treated with TMR-Lipo. Our data revealed that TMR-Lipo reduced the levels of TLR4- and RAGE-mediated downstream signaling molecules in a dose-dependent manner and decreased the endogenous levels of HMGB1 and PTX3 (Fig. 4C). Moreover, TMR-Lipo significantly reduced proinflammatory cytokines, including TNF- $\alpha$ , IL-6, and IL-12, while anti-inflammatory IL-10 increased (Fig. 4D). Collectively, our data demonstrated that TMR-Lipo modulates LPS-induced inflammatory responses in macrophages.

### 3.4. *In vitro* stability and pharmacokinetics of TMR-Lipo-Abs

Controlling both infection and inflammation are the two major goals of sepsis therapy. To accomplish these two goals simultaneously, the broad-spectrum antibiotics (Abs) ampicillin and gentamicin were introduced into the TMR-Lipo (denoted as TMR-Lipo-Abs) (Fig. 5A). TMR-Lipo-Abs were spherical, with a hydrodynamic particle size of approximately 109.05 nm and a PDI value of 0.236 (Fig. 5B), which was not significantly different from that of TMR-Lipo (Fig. 3B–C), implying that the loading of antibiotics into TMR-Lipo did not affect the physical characteristics. The entrapment efficiency is a drug loading rate of 30 mmol/L for Ampicillin and 2 mmol/L for Gentamicin in TMR-Lipo (Supporting Information Fig. S3). We also confirmed that TMR-Lipo-Abs had a negligible impact on the viability of BMDM cells (Fig. 5C) and the stability of TMR-Lipo-Abs showed no significant differences over the 8-day period (Supporting Information Fig. S4).

To elucidate the precise localization of TMR-Lipo-Abs in the organs, the bio-distribution of TMR-Lipo-Abs was assessed at each time point using *in vivo* imaging system (IVIS) imaging. As a result, high-contrast images of mice were captured 1–6 h after the administration of TMR-Lipo with IR783 *via* intraperitoneal delivery, revealing distribution primarily in the colon (Fig. 5D and E). Furthermore, we evaluated the pharmacodynamics of TMR-Lipo-Abs and IVIS imaging analysis showed that when TMR-Lipo-Abs was administered for three consecutive days in mice, 50% was retained at 96 h in the colon (Fig. 5F). Although the high-intensity signal observed in the peritoneal cavity and colon might be due to the intraperitoneal (IP) injection of TMR-Lipo-

Abs<sup>29</sup>, it is also expected that interactions with macrophages residing in the peritoneal cavity could contribute to this signal<sup>30</sup>.

Next, the *in vitro* metabolic stabilities and the pharmacokinetic parameters of TMR peptide, TMR-Lipo and TMR-Lipo-Abs were examined and the results are summarized in Fig. 5G. TMR-Lipo-Abs displayed excellent plasma stability and microsomal stabilities showing 100% and 96.8% remaining respectively 30 min after TMR-Lipo-Abs was treated with human plasma and human liver microsomes. The inhibitory activities of TMR-Lipo-Abs against most abundant five CYP isozymes were evaluated for examining the toxicity of its drug-drug interaction. The result showed that TMR-Lipo-Abs did not decrease the activity of all the tested CYP isozymes significantly. The pharmacokinetic parameters of TMR-Lipo-Abs on intraperitoneal administration in male C57BL/6 mice were observed. The AUC value and half-life indicated that TMR-Lipo-Abs was well maintained in the blood with effective drug concentration, which suggests that TMR-Lipo-Abs is suitable for *in vivo* experiment. Overall, we confirmed that TMR-Lipo-Abs has appropriate drug-like properties including *in vitro* stabilities and PK properties as well as pharmacological activities.

### 3.5. *In vivo* analysis of the therapeutic effect of TMR-Lipo on inflammation and sepsis

Based on their safety and immunomodulatory activity, the therapeutic efficacy of TMR-Lipo-Abs was evaluated using a cecal ligation and puncture (CLP)-induced polymicrobial sepsis model. CLP modeling in mice was conducted to induce mid- or high-grade sepsis, with the severity grade of sepsis being highly dependent on the position of cecal ligation<sup>31</sup>. As shown in Fig. 6A, in mid-grade CLP, mice treated with antibiotics alone exhibited approximately 50% mortality on Day 2 post-CLP surgery, which was lower than that in the TMR-Lipo-treated group (mortality >75% on Day 8). However, TMR-Lipo-Abs group, possessing both antimicrobial and immunomodulation capabilities, exhibited dose-dependent protection; 80% of the mice were protected from CLP-induced mortality after intraperitoneal injection of TMR-Lipo-Abs at a dose of 2 mg/kg per mouse. In high-grade CLP, treatment with antibiotics alone yielded comparable survival benefits to the CLP-PBS group, and mortality events in both the PBS and antibiotic groups were concentrated at 24–36 h post-CLP, which may be due to hyper-inflammatory reactions in the early-stage sepsis. Treatment with TMR-Lipo significantly improved survival rates compared with antibiotics alone, and the combination of the TMR peptide and antibiotics significantly reduced acute-phase mortality (Fig. 6B). Similarly, subcutaneous injection of TMR-Lipo into CLP mice at two time points (1 and 12 h) protected these mice from CLP-induced mortality (Fig. 6C). We confirmed that TMR-Lipo-antibiotics had synergistic effects in treating sepsis when combined with antibiotics used in preclinical or clinical studies (Supporting Information Fig. S5A and S5B). Notably, the long-term effects of TMR peptide treatment were confirmed not only for acute-phase mortality such as sepsis but also for Gram-negative *Pseudomonas aeruginosa* infection (Supporting Information Fig. S5C and S5D). These findings demonstrated that the TMR peptide can regulate acute-phase and long-term inflammation. Consistent with the mortality data, serum concentrations of the key inflammatory cytokines, including TNF- $\alpha$ , IL-6, and IL-12p40, significantly reduced in TMR-Lipo-Abs group, whereas there was no change in the level of IL-10 following TMR-Lipo-Abs treatment (Fig. 6D). As shown in Fig. 6E, TMR-Lipo-Abs decreased the expression of HMGB1 and



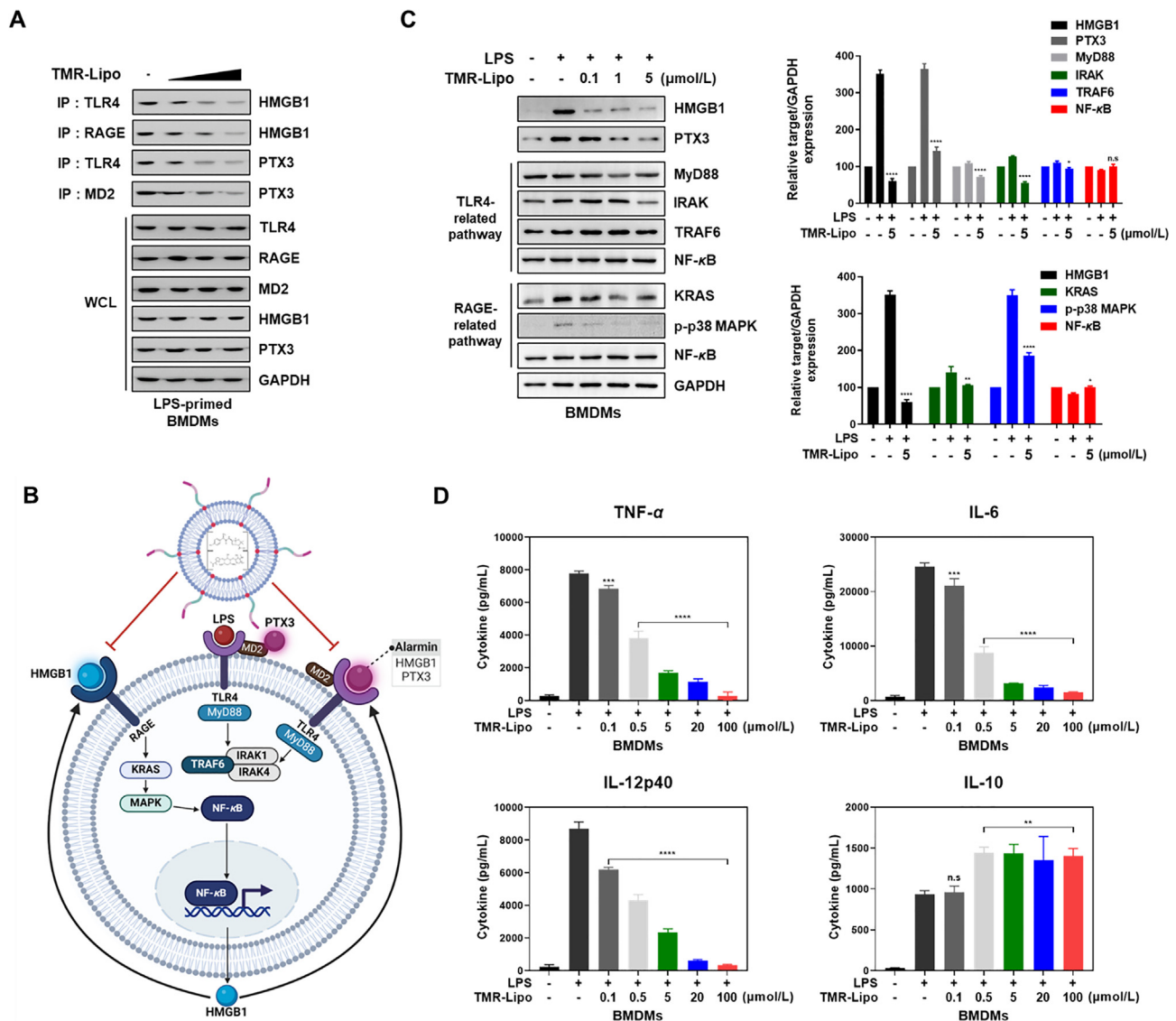


**Figure 4** Inhibitory effects of TMR-Lipo on TLR4/RAGE-mediated responses. (A) LPS-primed BMDMs (100 ng/mL LPS with 12 h) were treated with TMR-Lipo (0.1, 1, 5 μmol/L) for 12 h, followed by co-IP with αTLR4, αRAGE, or αMD2 and IB with indicated antibodies. (B) Schematic representation of TLR4 and RAGE signaling pathway and therapeutic targeting of TMR-Lipo (C) BMDMs were treated with TMR-Lipo as indicated concentrations (2 h), followed by treatment with LPS (100 ng/mL, 8 h). The amounts of HMGB1, PTX3, MyD88, IRAK, TRAF6, NF-κB, KRAS, and p-p38 were measured by IB in the whole cell lysates. GAPDH was used as a loading control. The data shown represent at least three independent experiments ( $n \geq 3$ ), and bars denote mean  $\pm$  SEM (\*\* $P < 0.01$ , \*\*\*\* $P < 0.001$ ), significance was measured by two-way ANOVA. n.s = not significant. (D) BMDMs were treated with TMR-Lipo (0.1, 0.5, 5, 20, or 100 μmol/L) in the presence LPS for 18 h. The secretion levels of TNF-α, IL-6, IL-12p40 and IL-10 were measured by ELISAs. The data shown represent at least three independent experiments ( $n \geq 3$ ), and bars denote mean  $\pm$  SEM (\*\* $P < 0.01$ , \*\*\*\* $P < 0.001$ ), significance was measured by two-way ANOVA. n.s = not significant.

PTX3 in the spleen, lungs, and liver of mice with sepsis. Moreover, histopathological analysis showed that treatment with TMR-Lipo-Abs significantly reduced the infiltration of immune cells and damage to the lungs, spleen, and liver compared to control septic mice (Fig. 6F). HMGB1 and PTX3 serve as proinflammatory cytokines that disseminate inflammation reactions through TLR4/RAGE binding, which is also a representative DAMP molecule indicating cell damage. Collectively, the histological and molecular analyses demonstrated that the synergistic combination of the TMR peptide and antibiotics mitigated excessive inflammation and prevented organ damage, enhancing the survival benefit of patients with sepsis.

#### 4. Discussion

The concomitant release of multiple alarmins and subsequent activation of the alarmin/PRR axis during sepsis perpetuate strong host inflammatory responses, suggesting that immunomodulation by targeting the alarmin/PRR axis is a promising approach for sepsis therapy. Here, we identified a TMR peptide system derived from HMGB1, PTX3-TLR4/MD2, or RAGE interactions, which specifically targets TLR4/MD2 and RAGE. Our study revealed that the TMR peptide significantly diminished TLR4- or RAGE-mediated secretion of proinflammatory cytokines by specifically

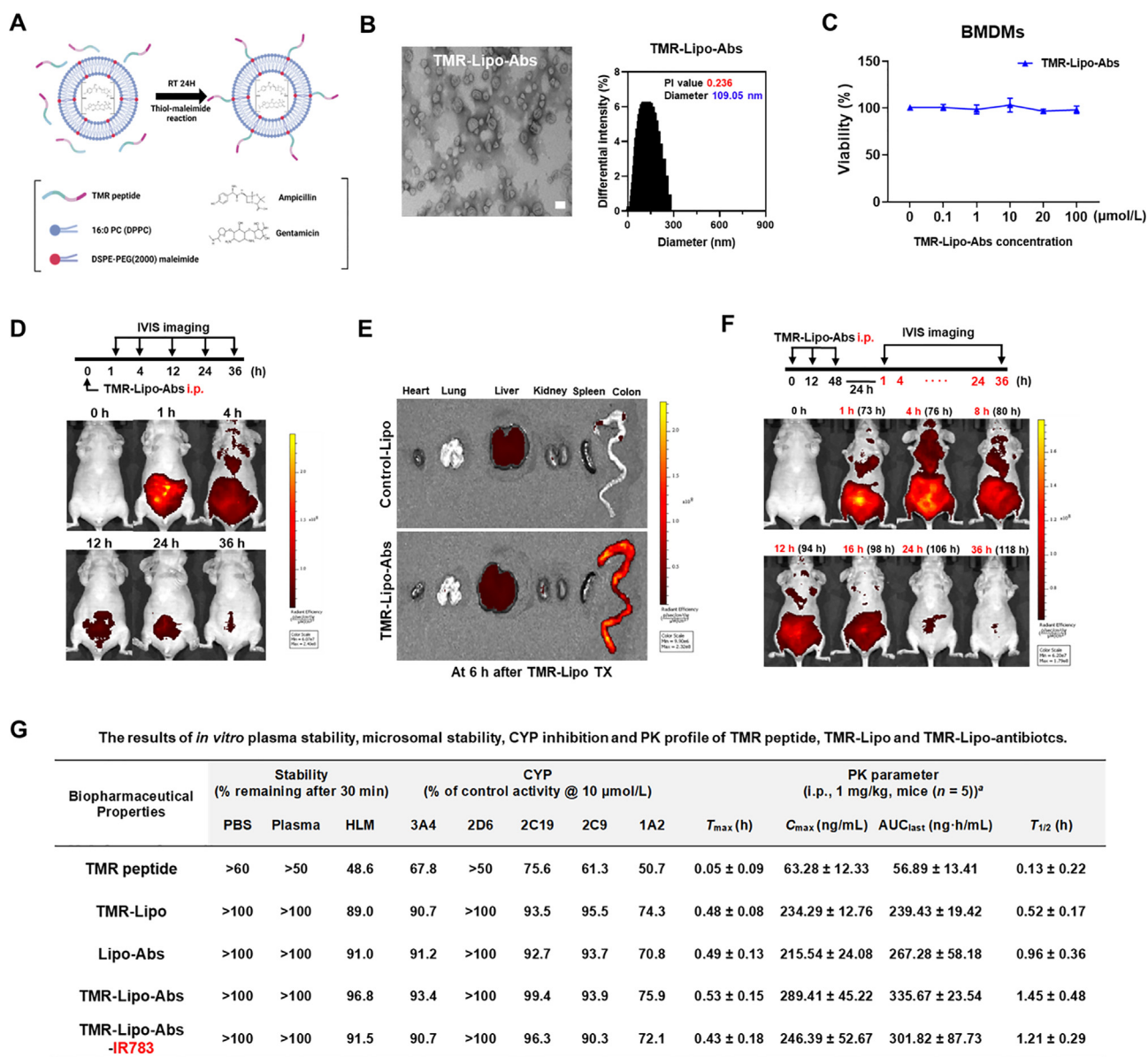


**Figure 5** Experimental characterization and effects drug-like properties of TMR-Lipo-Abs. (A, B) Preparation and characterization of TMR-Lipo-Abs. (A) Schematic design of antibiotics-loaded TMR-Lipo (TMR-Lipo-Abs). (B) TEM image (left) and Hydrodynamic particle size (right) of TMR-Lipo-Abs. Scale bars are 100 nm. (C) *In vitro* cytotoxicity of TMR-Lipo-Abs was evaluated for BMDMs. (D) *In vivo* bio-distribution analysis by IVIS imaging of TMR-Lipo with IR783. NIRF fluorescent images were taken at 1, 4, 12, 24, and 36 h after TMR-Lipo treatment. (E) 6 h after TMR-Lipo treatment, the mice were euthanized and dissected to capture ex-vivo NIR fluorescent images of the heart, lungs, liver, kidneys, spleen, and colon in that order. (F) NIRF fluorescent images were taken at various time points starting 24 h after TMR-Lipo treatment at 1, 12, and 48 h. (G) The results of *in vitro* plasma stability, microsomal stability, CYP inhibition and PK profile of TMR peptide, TMR-Lipo, Lipo-Abs, TMR-Lipo-Abs and TMR-Lipo-Abs-IR783. HLM, human liver microsomes; CYP, Cytochrome P450. <sup>a</sup> $T_{max}$ , time to reach;  $AUC_{last}$ , total area under the plasma concentration–time curve from time zero to last measured time;  $C_{max}$ , peak plasma concentration.

blocking HMGB1, PTX3 - TLR4/MD2, or RAGE interactions. Taken together, our data show that TMR peptides have protective effects against sepsis, as evidenced by the results of the CLP-induced sepsis model.

Sepsis is a disorder characterized by immune dysregulation initiated by infection. Therefore, modulating hyperinflammatory responses is as important as effective infection control in bacterial sepsis. In our CLP modeling studies, septic mice treated with antibiotics alone exhibited a modest survival benefit compared to PBS-treated septic mice (Fig. 6A-B), which is consistent with

findings showcasing the inadequacy of antibiotic treatment at achieving sepsis resolution<sup>32</sup>. Interestingly, treatment with TMR-Lipo-Abs, which possess both antibacterial and immunomodulatory capacities, significantly reduced acute-phase mortality in septic mice in a dose-dependent manner (Fig. 6A and B). Clinical studies have revealed that patients with sepsis have dynamic and dysregulated immune systems, underscoring the importance of precise immune modulation in sepsis treatment<sup>33</sup>. Considering the role of the alarmin-PRR axis in perpetuating inflammation during sepsis<sup>34</sup>, targeting the alarmin-PRR signaling axis provides an

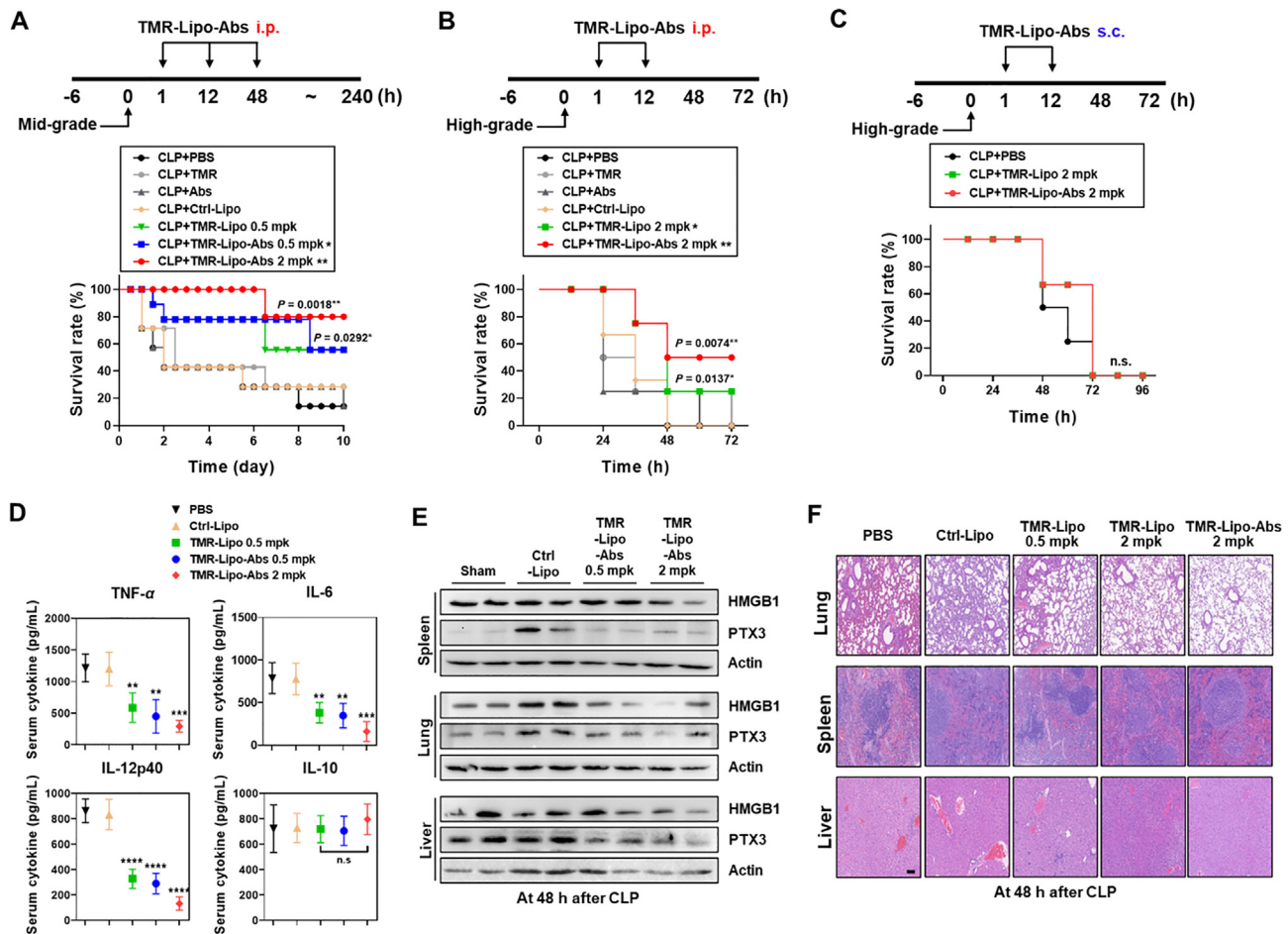


**Figure 6** TMR-Lipo-Abs protects mice from CLP-induced polymicrobial sepsis. (A–C) Schematic design of mid-grade (A) or high-grade (B, C) sepsis mouse model induced by cecal ligation and punctation (CLP) depending on the position of the cecal ligation (top). The survival of CLP mice treated with the indicated therapy was monitored for 10 days (A) or 72 h (B, C); mortality was measured for  $n = 10$  mice per group (bottom). Statistical differences compared with the PBS or TMR-Lipo-Abs-treated mice are indicated (log-rank test). The data are representative of three independent experimental replicates with similar results. (D) Serum cytokine levels. The data shown represent at least three independent experiments ( $n \geq 3$ ), significance was measured by Ordinary one-way ANOVA (TNF- $\alpha$ , \*\* $P = 0.0010$  and \*\*\* $P = 0.0002$ , IL-6, \*\* $P = 0.0057$  and \*\*\* $P = 0.0004$  and IL12p40, both \*\*\*\* $P < 0.0001$ ). n.s. = not significant. (E) IB identification and comparison of HMGB1 and PTX3 expression in spleen, lung, and liver cells of CLP mice after different treatment as a DAMP indicator for tissue damage. (F) Representative H&E staining of the lung, spleen, and liver from 3 mice per group. Scale bar, 100  $\mu$ m.

opportunity to develop novel therapeutic interventions for sepsis. Our developed TMR peptide is an antagonist of the alarmin-PRR axis that provides valuable insights into the modulation of hyperinflammation in sepsis and presents a potential therapeutic approach for sepsis treatment.

The release of HMGB1 into the circulation contributes to lethality in both endotoxemia and sepsis<sup>35</sup>. During lethal endotoxemia, HMGB1 binds to LPS<sup>36</sup>, forming HMGB1-LPS complexes that are taken up by phagocytes *via* TLR4 and RAGE<sup>37,38</sup>. Intracellular delivery of LPS activates caspase-11, a cytosolic endotoxin receptor, which subsequently induces pyroptosis<sup>39</sup>. The caspase-11-mediated pyroptosis, a lytic form of cell death, disrupts the intracellular niche and rapidly releases cell contents, such as DAMPs, which increase lethality in endotoxemia. Since extracellular LPS triggers pyroptosis of immune cells only after LPS has been delivered to caspase-11 inside the cell<sup>40,41</sup>, the role of these alarmin proteins in delivering LPS into the cytosol through TLR4/RAGE represents a potential therapeutic target to prevent lethality in sepsis<sup>42,43</sup>. A previous study

revealed that HMGB1 has binding regions for the lipid A moiety of LPS at amino acids 80–96<sup>44</sup>. In our study, domain mapping demonstrated that amino acids 89–98 of HMGB1 inhibited HMGB1-TLR4 interaction, and amino acid 160–169 of HMGB1 prevented HMGB1-RAGE interactions. These HMGB1-derived TLR4/RAGE targeted sequence may inhibit the delivery of LPS into the cytosol.

PTX3 is a multifunctional protein that plays a critical role in innate immune responses, regulating and amplifying inflammation. PTX3 expression increases in LPS-treated macrophages *via* the TLR4 and MyD88 pathway, promoting the production of inflammatory cytokines<sup>11</sup>. Additionally, PTX3 interacts with Fc gamma receptors and binds to MD2, a co-receptor of TLR4, thereby activating TLR4/MD2-mediated signal transduction and amplifying the inflammatory response. This action is further enhanced through caspase-11 dependent pyroptosis, leading to a robust inflammatory response in conditions such as sepsis<sup>24</sup>.

Oral delivery improves patient compliance; therefore, there is an increased interest in the development of systems that allow the oral

delivery of therapeutic peptides and proteins<sup>45,46</sup>. Further studies are warranted to determine the noninvasive delivery methods of TMR-Lipo-Abs to overcome the obstacles preceding its application for the treatment of sepsis. This study demonstrated the function of peptides in regulating innate immunity and provided a comprehensive description of the design, categorization, and application of peptide-based therapeutics for sepsis. Therapeutic peptides targeting macrophages-specific two receptors have several advantages, including economic benefits, feasibility of clinical-grade manufacturing, and applicability to sepsis therapy. By determining the impact of peptide length and formulation on their immunogenicity, we showed that peptide-based agents can be used and lead to major breakthroughs. Moreover, challenges remain in large-scale synthesis, safe delivery, and efficient immunotherapy to improve next-generation peptide-based immunotherapy.

The TMR-Lipo-Abs have a function of biologicals as potential therapeutics. However, these TMR-Lipo-Abs do not fulfil the requirements of direct antibiotics agent, which represent feasible alternatives to conventional chemotherapy to sepsis, due to the still unclear specificity and selectivity does not enable linking the effects of TMR-Lipo-Abs to host immune systems, as well as limitation of animal experimental model, unknown off-target effects, pharmacokinetics, safety data, and their potential feasibility for *in vivo* proof-of-concept studies. Further analyses are required to find out whether TMR-Lipo-Abs's can be translated to the *in vivo* situation or be observed in the presence of physiological condition to patient with sepsis.

In conclusion, these results pave the way for the development of an alarmin/PRR-targeting approach for sepsis. The macrophage-targeted delivery and specificity for immune cell type should be properly combined to maximize immunotherapeutic effects on sepsis, and future translational research and clinical trials are needed to promote peptide immunotherapeutics as next-generation sepsis immunotherapies. Increasing evidence indicates that the dysregulated release of alarmins is involved in uncontrolled processes observed in numerous inflammatory and autoimmune diseases, as well as in cancer. In addition to sepsis, the TMR peptide may potentially be applied as a potent immunomodulator in other inflammatory disorders, such as rheumatoid arthritis and inflammatory bowel disease.

### Acknowledgments

This work was supported by a National Research Foundation of Korea grant funded by the Korean government (MSIP) (grant Nos. 2019R1I1A2A01064237 and 2021R1A4A5032463 to Chul-Su Yang) and a grant from the Korea Health Technology R&D Project through the Korea Health Industry Development Institute (KHIDI) funded by the Ministry of Health & Welfare, Republic of Korea (HI22C0884 to Chul-Su Yang). SJM was supported by the Health Fellowship Foundation (to Seok-Jun Mun, Republic of Korea). We would like to thank all the members of the Infection Biology Lab for critically reading and discussing this manuscript.

### Author contributions

Seok-Jun Mun: Methodology, Investigation. Euni Cho: Methodology, Investigation. Woo Jin Gil: Methodology, Investigation. Seong Jae Kim: Methodology, Investigation. Hyo Keun Kim: Methodology, Investigation. Yu Seong Ham: Methodology,

Investigation. Chul-Su Yang: Writing – review & editing, Writing – original draft, Validation, Supervision.

### Conflicts of interest

The authors declare that this study was conducted in the absence of any commercial or financial relationships that could be construed as potential conflicts of interest.

### Appendix A. Supporting information

Supporting information to this article can be found online at <https://doi.org/10.1016/j.apsb.2024.08.015>.

### References

- Hotchkiss RS, Moldawer LL, Opal SM, Reinhart K, Turnbull IR, Vincent JL. Sepsis and septic shock. *Nat Rev Dis Primers* 2016;**2**:16045.
- Singer M, Deutschman CS, Seymour CW, Shankar-Hari M, Annane D, Bauer M, et al. The third international consensus definitions for sepsis and septic shock (sepsis-3). *JAMA* 2016;**315**:801–10.
- Delano MJ, Ward PA. The immune system's role in sepsis progression, resolution, and long-term outcome. *Immunol Rev* 2016;**274**:330–53.
- Medzhitov R, Janeway C. Innate immunity. *N Engl J Med* 2000;**343**:338–44.
- Hensler T, Sauerland S, Bouillon B, Raum M, Rixen D, Helling HJ, et al. Association between injury pattern of patients with multiple injuries and circulating levels of soluble tumor necrosis factor receptors, interleukin-6 and interleukin-10, and polymorphonuclear neutrophil elastase. *J Trauma* 2002;**52**:962–70.
- Hotchkiss RS, Karl IE. The pathophysiology and treatment of sepsis. *N Engl J Med* 2003;**343**:138–50.
- Reinhart K, Karzai W. Anti-tumor necrosis factor therapy in sepsis: update on clinical trials and lessons learned. *Crit Care Med* 2001;**29**:S121–5.
- Wang H, Bloom O, Zhang M, Vishnubhakat JM, Ombrellino M, Che J, et al. HMG-1 as a late mediator of endotoxin lethality in mice. *Science* 1999;**285**:248–51.
- Peltz ED, Moore EE, Eckels PC, Damle SS, Tsuruta Y, Johnson JL, et al. HMGB1 is markedly elevated within 6 hours of mechanical trauma in humans. *Shock* 2009;**32**:17–22.
- Lutterloh EC, Opal SM, Pittman DD, Keith JC, Tan XY, Clancy BM, et al. Inhibition of the RAGE products increases survival in experimental models of severe sepsis and systemic infection. *Crit Care* 2007;**11**:R122.
- Abeyama K, Stern DM, Ito Y, Kawahara K, Yoshimoto Y, Tanaka M, et al. The N-terminal domain of thrombomodulin sequesters high-mobility group-B1 protein, a novel antiinflammatory mechanism. *J Clin Invest* 2005;**115**:1267–74.
- Kim JS, Cho E, Mun SJ, Kim S, Kim SY, Kim DG, et al. Multifunctional MPT protein as a therapeutic agent against *Mycobacterium tuberculosis*. *Biomedicines* 2021;**9**:545.
- Cho E, Mun SJ, Jeon M, Kim HK, Baek H, Ham YS, et al. Tumor-targeted liposomes with platycodin D2 promote apoptosis in colorectal cancer. *Mater Today Bio* 2023;**22**:100745.
- Oswald M, Geissler S, Goepperich A. Determination of the activity of maleimide-functionalized phospholipids during preparation of liposomes. *Int J Pharm* 2016;**514**:93–102.
- Cai X, Bandla A, Chuan CK, Magarajah G, Liao LD, The DBL, et al. Identifying glioblastoma margins using dual-targeted organic nanoparticles for efficient *in vivo* fluorescence image-guided photothermal therapy. *Mater Horizons* 2019;**6**:311–7.

16. Schumacher I, Margalit R. Liposome-encapsulated ampicillin: physicochemical and antibacterial properties. *J Pharm Sci* 1997;**86**: 635–41.
17. Alhariri M, Majrashi MA, Bahkali AH, Almajed FS, Azghani AO, Khiyami MA, et al. Efficacy of neutral and negatively charged liposome-loaded gentamicin on planktonic bacteria and biofilm communities. *Int J Nanomed* 2017;**12**:6949–61.
18. Swenson CE, Stewart KA, Hammett JL, Fitzsimmons WE, Ginsberg RS. Pharmacokinetics and *in vivo* activity of liposome-encapsulated gentamicin. *Antimicrob Agents Chemother* 1990;**34**: 235–40.
19. Lee D, Lee E, Jang S, Kim K, Cho E, Mun SJ, et al. Discovery of *Mycobacterium tuberculosis* Rv3364c-derived small molecules as potential therapeutic agents to target SNX9 for sepsis. *J Med Chem* 2022;**65**:386–408.
20. Pineda LC, Watt KM. New antibiotic dosing in infants. *Clin Perinatol* 2015;**42**:167–76.
21. Sommer R, Eitelberger F, Hohenauer L. Gentamicin dosage in newborn infants. *Klin Padiatr* 1989;**201**:387–92.
22. Lee YT, Gong M, Chau A, Wong WT, Bazoukis G, Wong SH, et al. International Health Informatics Study, Pentraxin-3 as a marker of sepsis severity and predictor of mortality outcomes: a systematic review and meta-analysis. *J Infect* 2018;**76**:1–10.
23. Amiot F, Fitting C, Tracey KJ, Cavaillon JM, Dautry F. Lipopolysaccharide-induced cytokine cascade and lethality in  $LT\alpha/TNF\alpha$ -deficient mice. *Mol Med* 1997;**3**:864–75.
24. Bozza S, Campo S, Arseni B, Inforzato A, Ragnar L, Bottazzi B, et al. PTX3 binds MD-2 and promotes TRIF-dependent immune protection in aspergillosis. *J Immunol* 2014;**193**:2340–8.
25. Harris HE, Andersson U, Pisetsky DS. HMGB1: a multifunctional alarmin driving autoimmune and inflammatory disease. *Nat Rev Rheumatol* 2012;**8**:195–202.
26. Cho E, Mun SJ, Kim HK, Ham YS, Gil WJ, Yang CS. Colon-targeted S100A8/A9-specific peptide systems ameliorate colitis and colitis-associated colorectal cancer in mouse models. *Acta Pharmacol Sin* 2024;**45**:581–93.
27. Lombardo D, Kiselev MA. Methods of liposomes preparation: formation and control factors of versatile nanocarriers for biomedical and nanomedicine application. *Pharmaceutics* 2022;**14**:543.
28. Hodgins NO, Al-Jamal WT, Wang JT, Klippstein R, Costa PM, Sosabowski JK, et al. Investigating *in vitro* and *in vivo* alphavbeta6 integrin receptor-targeting liposomal alendronate for combinatory gammadelta T cell immunotherapy. *J Control Release* 2017;**256**: 141–52.
29. Dou S, Smith M, Wang Y, Rusckowski M, Liu G. Intraperitoneal injection is not always a suitable alternative to intravenous injection for radiotherapy. *Cancer Biother Radiopharm* 2013;**28**:335–42.
30. Honda M, Kadohisa M, Yoshii D, Komohara Y, Hibi T. Directly recruited GATA6<sup>+</sup> peritoneal cavity macrophages contribute to the repair of intestinal serosal injury. *Nat Commun* 2021;**12**:7294.
31. Rittirsch D, Huber-Lang MS, Flierl MA, Ward PA. Immunodesign of experimental sepsis by cecal ligation and puncture. *Nat Protoc* 2009;**4**: 31–6.
32. Halbach JL, Wang AW, Hawisher D, Cauvi DM, Lizardo RE, Rosas J, et al. Why antibiotic treatment is not enough for sepsis resolution: an evaluation in an experimental animal model. *Infect Immun* 2017;**85**: e00664-17.
33. Yao RQ, Ren C, Zheng LY, Xia ZF, Yao YM. Advances in immune monitoring approaches for sepsis-induced immunosuppression. *Front Immunol* 2022;**13**:891024.
34. Li L, Lu YQ. The regulatory role of high-mobility group protein 1 in sepsis-related immunity. *Front Immunol* 2020;**11**:601815.
35. Lamkanfi M, Sarkar A, Vande Walle L, Vitari AC, Amer AO, Wewers MD, et al. Inflammasome-dependent release of the alarmin HMGB1 in endotoxemia. *J Immunol* 2010;**185**:4385–92.
36. Youn JH, Oh YJ, Kim ES, Choi JE, Shin JS. High mobility group box 1 protein binding to lipopolysaccharide facilitates transfer of lipopolysaccharide to CD14 and enhances lipopolysaccharide-mediated TNF-alpha production in human monocytes. *J Immunol* 2008;**180**:5067–74.
37. Wang J, Li R, Peng Z, Hu B, Rao X, Li J. HMGB1 participates in LPS-induced acute lung injury by activating the AIM2 inflammasome in macrophages and inducing polarization of M1 macrophages via TLR2, TLR4, and RAGE/NF-kappaB signaling pathways. *Int J Mol Med* 2020;**45**:61–80.
38. Deng M, Tang Y, Li W, Wang X, Zhang R, Zhang X, et al. The endotoxin delivery protein HMGB1 mediates caspase-11-dependent lethality in sepsis. *Immunity* 2018;**49**:740–53.
39. Rathinam VAK, Zhao Y, Shao F. Innate immunity to intracellular LPS. *Nat Immunol* 2019;**20**:527–33.
40. Hagar JA, Powell DA, Aachoui Y, Ernst RK, Miao EA. Cytoplasmic LPS activates caspase-11: implications in TLR4-independent endotoxic shock. *Science* 2013;**341**:1250–3.
41. Cheng KT, Xiong S, Ye Z, Hong Z, Di A, Tsang KM, et al. Caspase-11-mediated endothelial pyroptosis underlies endotoxemia-induced lung injury. *J Clin Invest* 2017;**127**:4124–35.
42. Piccinini AM, Midwood KS. DAMPening inflammation by modulating TLR signalling. *Mediators Inflamm* 2010;**2010**:672395.
43. Weinhage T, Wirth T, Schutz P, Becker P, Lueken V, Skryabin BV, et al. The receptor for advanced glycation endproducts (RAGE) contributes to severe inflammatory liver injury in mice. *Front Immunol* 2020;**11**:1157.
44. Youn JH, Kwak MS, Wu J, Kim ES, Ji Y, Min HJ, et al. Identification of lipopolysaccharide-binding peptide regions within HMGB1 and their effects on subclinical endotoxemia in a mouse model. *Eur J Immunol* 2011;**41**:2753–62.
45. Islam MM, Raikwar S. Enhancement of oral bioavailability of protein and peptide by polysaccharide-based nanoparticles. *Protein Pept Lett* 2024;**31**:209–28.
46. Peng H, Wang J, Chen J, Peng Y, Wang X, Chen Y, et al. Challenges and opportunities in delivering oral peptides and proteins. *Expert Opin Drug Deliv* 2023;**20**:1349–69.